



HAL
open science

First record of Sivameryx (Cetartiodactyla, Anthracotheriidae) from the lower Miocene of Israel highlights the importance of the Levantine Corridor as a dispersal route between Eurasia and Africa

Ari Grossman, Ran Calvo, Raquel López-Antoñanzas, Fabien Knoll, Gideon Hartman, Rivka Rabinovich

► **To cite this version:**

Ari Grossman, Ran Calvo, Raquel López-Antoñanzas, Fabien Knoll, Gideon Hartman, et al.. First record of Sivameryx (Cetartiodactyla, Anthracotheriidae) from the lower Miocene of Israel highlights the importance of the Levantine Corridor as a dispersal route between Eurasia and Africa. *Journal of Vertebrate Paleontology*, 2019, 39 (2), pp.e1599901. 10.1080/02724634.2019.1599901 . hal-02365607

HAL Id: hal-02365607

<https://hal.science/hal-02365607>

Submitted on 16 Dec 2020

HAL is a multi-disciplinary open access archive for the deposit and dissemination of scientific research documents, whether they are published or not. The documents may come from teaching and research institutions in France or abroad, or from public or private research centers.

L'archive ouverte pluridisciplinaire **HAL**, est destinée au dépôt et à la diffusion de documents scientifiques de niveau recherche, publiés ou non, émanant des établissements d'enseignement et de recherche français ou étrangers, des laboratoires publics ou privés.



First description of *Sivameryx* (Cetartiodactyla: Anthracotheriidae) from the Early Miocene of Israel highlights the importance of the Levantine Corridor as a dispersal route between Eurasia and Africa

Journal:	<i>Journal of Vertebrate Paleontology</i>
Manuscript ID	JVP-2018-0083.R3
Manuscript Type:	Article
Date Submitted by the Author:	11-Mar-2019
Complete List of Authors:	Grossman, Aryeh; Midwestern University, Anatomy; Midwestern University, College of Veterinary Medicine; Midwestern University, Arizona College of Osteopathic Medicine Calvo, Ran; Geological Survey of Israel López-Antoñanzas, Raquel; Institut des Sciences de l'Évolution de Montpellier, Université Montpellier, CNRS, IRD, EPHE. Knoll, Fabien; Fundación Conjunto Paleontológico de Teruel-Dinópolis, ; University of Manchester, School of Earth & Environmental Sciences, Hartman, Gideon; University of Connecticut, Anthropology Rabinovich, Rivka; The Hebrew University of Jerusalem, National Natural History Collections, Institute of Earth Sciences, Institute of Archaeology,
Key Words:	Israel, early Miocene, anthracotheriidae, cetartiodactyla, <i>Sivameryx</i> , Levantine corridor

SCHOLARONE™
Manuscripts

1
2
3 1 First **description** of *Sivameryx* (Cetartiodactyla, Anthracotheriidae) from the Early Miocene of
4
5
6 2 Israel highlights the importance of the Levantine Corridor as a dispersal route between Eurasia
7
8 3 and Africa
9

10
11 4 ARI GROSSMAN, *,^{1,2,3} RAN CALVO,⁴ RAQUEL LOPEZ-ANTONANZAS,⁵ FABIEN KNOL,^{6,7} GIDEON
12
13
14 5 HARTMAN,^{8,9} and RIVKA RABINOVICH¹⁰
15

16
17 6 ¹Department of Anatomy, College of Graduate Studies, Midwestern University, Glendale, AZ
18
19 7 85308, USA, agross@midwestern.edu;
20
21

22 8 ²College of Veterinary Medicine, Midwestern University, Glendale, AZ 85308, USA;
23
24

25 9 ³Arizona College of Osteopathic Medicine, Midwestern University, Glendale, AZ 85308, USA;
26
27

28 10 ⁴Geological Survey of Israel, Jerusalem, Israel;
29
30

31 11 ⁵Institut des Sciences de l'Évolution de Montpellier (ISE - M, UMR 5554, CNRS/UM/IRD/EPHE),
32
33
34 12 c.c. 64, Université de Montpellier, Place Eugène Bataillon, F -34095 Montpellier Cedex 05,
35
36
37 13 France;
38

39 14 ⁶ARAID—Fundación Conjunto Paleontológico de Teruel-Dinópolis, 44002, Teruel, Spain;
40
41
42

43 15 ⁷School of Earth and Environmental Sciences, University of Manchester, Manchester, M13 9PL,
44
45 16 United Kingdom;
46
47

48 17 ⁸Department of Anthropology, University of Connecticut, Unit 1176, 354 Mansfield Road,
49
50
51 18 Storrs, CT 06269, USA;
52
53
54

55
56 * Corresponding author
57

1
2
3 19 ⁹Center for Environmental Sciences and Engineering, University of Connecticut, 3107 Horsebarn
4
5
6 20 Hill Road, Building 4 room 10, Storrs, CT 06269, USA;
7

8
9 21 ¹⁰National Natural History Collections, Institute of Earth Sciences, Institute of Archaeology, The
10
11 22 Hebrew University of Jerusalem, Berman Building, Edmond J. Safra Campus, Givat Ram,
12
13 23 Jerusalem 91904, Israel
14
15

16
17 24
18

19
20 25 RH: GROSSMAN ET AL.—FIRST ANTHRACOTHERE FROM ISRAEL
21
22

23 26
24
25
26
27
28
29
30
31
32
33
34
35
36
37
38
39
40
41
42
43
44
45
46
47
48
49
50
51
52
53
54
55
56
57
58
59
60

1
2
3 27 ABSTRACT—The genus *Sivameryx* (Cetartiodactyla: Anthracotheriidae), found both in Asia and
4
5
6 28 Africa, is considered of Asian origin. Recent excavations in the Negev region of southern Israel
7
8 29 led to the discovery of a new Early Miocene site called Kamus Junction. Among the fossils
9
10
11 30 recovered at Kamus Junction is an upper molar of *Sivameryx palaeindicus*. Although known
12
13 31 species of *Sivameryx* have often been distinguished by size, comparisons of the new specimen
14
15 32 with known *Sivameryx* teeth from Asia and Africa emphasize the need for caution when
16
17
18 33 assigning *Sivameryx* fossils to species based on size alone. This record of *Sivameryx* highlights
19
20 34 the importance of the Levant as a corridor connecting Eurasia and Africa. The new find, along
21
22
23 35 with other recent finds, demonstrates that the Levantine Corridor facilitated faunal dispersal
24
25 36 events that shaped modern biotas as early as the Early Miocene.

37

38 INTRODUCTION

39
40 Multiple mammalian orders and families appear to have migrated from Africa to Eurasia
41 during the Early and Middle Miocene in a series of relatively rapid migration events (e.g. [Cote et al., 2018](#);
42 [Leakey et al., 2011](#)). An uncertain but substantial number of African taxa such as
43 proboscideans migrated out of Africa roughly simultaneously (e.g. [Sanders et al., 2010](#);
44 [Sanders and Miller, 2002](#)). Direct fossil evidence for these migrations from sites that lie between Africa
45 and Eurasia are rare but crucial for reconstructing biogeographic patterns of dispersal. The
46 Levantine Corridor, located between Africa and Eurasia, provides the best case for studying
47 such patterns ([Tchernov et al., 1987](#)). Preliminary descriptions recognized 19 fossil Early

1
2
3 48 Miocene mammal taxa from the Negev of Israel (Goldsmith et al., 1982; Savage and Tchernov,
4
5 49 1968; Tchernov et al., 1987). These taxa were primarily of African affinities but demonstrated
6
7
8 50 high levels of regional endemism, which, the authors argued, were probably indicative of
9
10
11 51 environmental and not temporal differences with other sites in Africa and Asia (Tchernov et al.,
12
13 52 1987).

14
15
16 53 Anthracotheres are relatively common in the Early Miocene fossil record of East and
17
18 54 North Africa (Evans et al., 1981; Leakey et al., 2011; Rowan et al., 2015) as well as Eurasia
19
20
21 55 (Antoine et al., 2013; Ducrocq and Lihoreau, 2006; Lihoreau and Ducrocq, 2007; Patnaik, 2013;
22
23 56 Savage et al., 1977; Sehgal and Bhandari, 2014) . Because anthracotheres are so widely
24
25
26 57 dispersed, paleontologists often regard them as useful indicators of early phases of
27
28 58 intercontinental dispersal events (e.g. Lihoreau and Ducrocq, 1995; Holroyd et al., 2010).
29
30
31 59 Anthracotheres appear in the early reports of mammals from the Miocene of Israel (Goldsmith
32
33 60 et al., 1982; Savage and Tchernov, 1968), and Goldsmith even named the main Early Miocene
34
35
36 61 locality from the Negev "Anthracothere Hill" (Goldsmith et al., 1988). However, the only formal
37
38 62 description of the Miocene mammals of the Negev in Israel, Tchernov et al. (1987: Table 7) does
39
40
41 63 not mention anthracotheres. Here we formally describe anthracothere remains from Israel for
42
43 64 the first time, specifically the material found at Kamus Junction.

44
45
46 65 In 2012, we began surveying and excavating new localities in Israel to reconstruct the
47
48 66 landscape and biota of the Levantine Corridor during the Miocene (López-Antoñanzas et al.,
49
50
51 67 2014; López-Antoñanzas et al., 2016; Rabinovich et al., 2014). During excavation of Kamus
52
53
54 68 Junction, a new Early Miocene locality, new specimens were recovered including

1
2
3 69 proboscideans, a giraffid (*Canthumeryx* sp.), and one anthracothere tooth, which we describe
4
5
6 70 here.

7
8
9 71

12 72 **Location and Geological Setting of Kamus Junction Locality**

13
14
15 73 The Kamus Junction (KJ) locality is located at the southwestern side of the Yamin Plain, in
16
17
18 74 the northern Negev desert of Israel. The KJ sediments were deposited in the Miocene Hazeva
19
20
21 75 Formation. During most of the Early and Middle Miocene, the Neo-Tethys shoreline was located
22
23 76 in Be'er Sheva area (Gvirtzman and Buchbinder, 1969), with the site some 30km southeast (Fig.
24
25 77 1).

26
27
28 78 During the Early Miocene large drainage systems flowed from deep-inland areas of the
29
30
31 79 Arabian Plate, in the southeast, toward the Neo-Tethys, in the northwest. The Hazeva Formation
32
33
34 80 consists mostly of fluvial, fine to coarse, sandstones, with some shale and conglomerates.
35
36
37 81 Episodically, lacustrine environments prevailed, and marls and limestone were also deposited
38
39 82 (Calvo and Bartov, 2001). Remnants of the Miocene fluvial-lacustrine Hazeva Formation are
40
41
42 83 preserved in the northern Negev in Israel in synclinal basins within the folds of the 'Syrian Arc'
43
44 84 folds system (Zilberman and Calvo, 2013) (Fig. 1). Several large unconformities separate the
45
46 85 members in the formation (Fig. 2). In the Yamin Plain, the upper parts of the Zefa Member coat
47
48 86 the basin edge, and are covered by cycles of layers of the Rotem Member (Fig. 1C, E). The Rotem
49
50
51 87 Member, with a thickness of up to 1,000 m in the Arava Valley, contains low- as well as high-
52
53 88 energy alluvial facies represented by conglomerate-sand-silt-clay cycles. Due to unconformities,
54
55
56 89 during- and post-Hazeva time, only ~50m of the Rotem Member are preserved in Yamin Plain. In

1
2
3 90 KJ locality the lower part of the Rotem Member begins with 10m of coarse sandstone layers with
4
5
6 91 cross-bedding, followed by 15m of alternating sandstone and shale-marls layers (Fig. 1E). The
7
8 92 upper section begins with 1m thick gritstone, which continues into friable sandstone with
9
10
11 93 petrified tree-trunks. HUJI KJ 31 was found eroding out of the sandstone along with fossils of
12
13 94 other mammals, crocodylians and turtles.
14
15
16
17
18
19

20 96 **Age of Kamus Junction (KJ)**

21
22
23 97 Due to the absence of radiometric dateable markers within the Hazeva Formation, only its
24
25 98 base and top ages are known. In central Sinai (Egypt) conglomerate of the base of the formation
26
27 99 overlay dikes of ~25 Ma (K-Ar ages) (Steinitz et al., 1978), while in Jordan (east of the Yamin Plain)
28
29 100 a ~20 Ma dike cuts the same stratigraphic unit (Calvo, 2000), indicating that the lower parts of
30
31
32 101 the Hazeva Formation were likely deposited during the late Oligocene or Early Miocene (Calvo
33
34
35 102 and Bartov, 2001). Based on geomorphological relationship between marine invasion and
36
37 103 terrestrial erosional episodes in Be'er Sheva area, Bar and Zilberman (2016) concluded that the
38
39
40 104 Hazeva Formation deposition ended before ~16-14 Ma.
41
42
43
44
45

46 106 **Dental terminology**—mostly follows Boisserie et al. 2010 and Bärmann and Rössner. 2011.
47
48
49
50 107
51
52

53 108 SYSTEMATIC PALEONTOLOGY
54
55
56
57
58
59
60

109

110 CETARTIODACTYLA Montgelard et al. 1997

111 ANTHRACOTHERIIDAE Leidy 1869

112 BOTHRIODONTINAE Scott, 1940

113 MERYCOPOTAMINI Lydekker, 1883

114 *SIVAMERYX* Lydekker, 1877115 Type-species *Sivameryx palaeindicus* Lydekker, 1877116 (included species: *S. africanus* Andrews 1914; *S. moneyi* Fourteau 1918)

117 Stratigraphic range: Early Miocene

118 **Diagnosis**—Following Pickford (1991); Lihoreau (2003), Holroyd et al. (2010), Lihoreau
 119 et al. (2016). Medium to small in size; canines sexually dimorphic; p1 double rooted; lower
 120 molars selenodont with anterior crests of labial cusps reaching lingual surface of crown, often
 121 ending in a small cuspule; four crests from the metaconid; lingual cusps of lower molars
 122 mediolaterally compressed; talonid of m3 loop-like and strongly obliquely oriented; upper
 123 molars with four main cusps and a paraconule almost fused with protocone and of similar
 124 height (=quasi-pentacuspitate); looplike parastyles and mesostyles; two distal crests from
 125 protocone; symphysis reaches back to level of p1; no genial spine; postcanine diastema long,
 126 with a flange-like protuberance leaning laterally; enamel microstructure is a mono-zonal radial
 127 Schmelzmuster (not equivalent to the cetartiodactyl plesiomorph condition).

1
2
3 128 **New Material**—HUJI KJ 31: Right second molar (M2) (Fig. 2)
4
5

6 129 **Comparative Description**—the tooth is a nearly complete crown with a slightly broken
7
8
9 130 anterior (=mesial) cingulum and the anterior part of the roots also sheared. The molar is bucco-
10
11 131 lingually (21.8mm) wider than it is mesio-distally long (19.8mm). The crown is brachyodont and
12
13
14 132 the cusps are selenodont and high, giving the crown a tall appearance. There are four main
15
16 133 cusps (paracone, protocone, metacone, metaconule), and a fifth very small paraconule, a
17
18 134 distinctive character of *Sivameryx* referred to as quasi-pentacuspitate by some authors
19
20 135 (Holroyd et al., 2010; Pickford, 1991). The tips of the metacone and the paracone of HUJI KJ 31
21
22 136 pinch-in so that the tips of the cusps are close together. This pinching exaggerates the sloping
23
24 137 of the buccal sides of each buccal cusp contrasting with the less sloped lingual sides of the
25
26 138 lingual cusps. This is especially visible in the metacone. A looping mesostyle connects the
27
28 139 two buccal cusps. The parastyle is partially broken but was clearly also looping and prominent.
29
30 140 The metastyle of HUJI KJ 31 is relatively smaller than the mesostyle or parastyle. The
31
32 141 preparacristule is broad but slightly abraded. It wraps around the mesiolingual side of the
33
34 142 paracone to merge with the parastyle. Both the metacone and the paracone have distinct
35
36 143 bulbous ribs descending buccally; that of the paracone appears larger although this could be an
37
38 144 artefact of the degree of erosion of the metacone. A median transverse valley separates the
39
40 145 mesial and distal portions of the tooth. The narrow base of the valley is approximately at the
41
42 146 level of the cervix of the tooth. The median transverse valley is enclosed buccally by the
43
44 147 mesostyle, and continues lingually to terminate at the lingual cingulum. The mesial cingulum
45
46 148 begins at the mesial end of the parastyle where the preparacristule merges with the paracone.
47
48 149 The mesial cingulum is continuous with a very prominent and arcuate cingulum that surrounds
49
50
51
52
53
54
55
56
57
58
59
60

1
2
3 150 the protocone lingually. This protocone cingulum merges with a second arcuate cingulum that
4
5
6 151 surrounds the metaconule, and the two cingula meet at the termination of the median
7
8 152 transverse valley. The metaconule cingulum is continuous with a distal cingulum that extends to
9
10
11 153 the distal part of the metastyle. Thus, the cingula form a single, shelf-like cingulum covering all
12
13 154 but the buccal aspect of the tooth.

14
15
16 155 HUJI KJ 31 shares with other bothriodontine anthracotheres an upper molar mesostyle
17
18 156 invaded by the median transverse valley and selenodont crescentric cusps. Anthracotheriinae
19
20
21 157 differ by their accessory protostyle on the mesial cingulum, and relatively bunodont upper
22
23
24 158 molar cusps. Micorbunodontinae differ because they lack the median transverse valley invading
25
26 159 the mesostyle,

27
28
29 160 Members of the tribe Merycopotamini (*Afromeryx*, *Sivameryx*, *Hemimeryx*,
30
31 161 *Merycopotamus*, *Libycosaurus*) are distinguished in their upper molars from other
32
33
34 162 bothriodontine anthracotheres by a preparacrista that connects labially with the parastyle, lack
35
36
37 163 of ectocristyle, and development of the molar entostyle (Lihoreau et al., 2016). All characters
38
39 164 observed in HUJI KJ 31. We thus restrict further comparisons primarily to Merycopotamini with
40
41
42 165 a few additions.

43
44
45 166 We place HUJI KJ 31 in *Sivameryx* because it is a five-cusped upper molar with a reduced
46
47 167 paraconule (i.e. quasi-pentascuspidate). It also shares with *Sivameryx* a loop-like mesostyle and
48
49
50 168 a strongly developed lingual cingulum of the protocone.

1
2
3 169 *Brachyodus* (Early Miocene of Africa and Europe, Middle Miocene of Thailand) differs
4
5
6 170 from HUJI KJ 31 because it has pinched rather than looping styles on its upper molars.

7
8 171 *Brachyodus* is also much bigger than HUJI KJ 31.
9

10
11 172 *Afromeryx* (Early Miocene of East and North Africa), *Hemimeryx* (Late Oligocene to late
12
13 Early Miocene of Pakistan), *Telmatodon* (Early Miocene of Palistan), *Gonotelma* (*Libycosaurus*
14 173
15
16 174 (Late Miocene of North Africa and Uganda), and *Merycompotamus* (late Middle Miocene to
17
18 Late Miocene of India and Pakistan) differ from HUJI KJ 31 because they are tetracuspitate and
19 175
20
21 176 their upper molars lack a paraconule.

22
23
24 177 *Elomeryx*, a bothriodontine genus with a widespread Eurasian and North American
25
26
27 178 distribution differs from HUJI KJ 31, by its much more developed paraconule, which is located
28
29 179 substantially farther from the protocone than seen in *Sivameryx*.
30

31
32
33 180 We recognize HUJI KJ 31 as a second upper molar (M2). The tooth has a distal wear
34
35 181 facet indicating that it is not an M3. Furthermore, the marked pinching of the tips of the
36
37 182 metacone and the paracone causing exaggerated sloping of the buccal sides of each buccal cusp
38
39 183 is particularly exaggerated on the metacone of HUJI KJ 31, a condition typically more marked on
40
41 184 M1 and M2. To determine if it is a first or second upper molar, we collected all available mesio-
42
43 185 distal length and bucco-lingual width measurements of upper molars assigned to *Sivameryx*
44
45 186 (Table 1). We used a simple bi-variate plot to compare HUJI KJ 31 with the other upper molars
46
47 187 belonging to *Sivameryx* species (Fig. 3). Recent discoveries of skulls of *S. africanus* (Rowan et al.,
48
49 188 2015) and *S. moneyi* (Miller et al., 2014) demonstrate that in both *S. africanus* and *S. moneyi*
50
51 189 the M1 is smaller than M2 and M3. The M2 and M3 overlap in size although the M3 is generally
52
53
54
55
56
57
58
59
60

1
2
3 190 larger than M2 (Fig. 3). HUJI KJ 31 falls within the cluster that includes M2 of *S. africanus*, *S.*
4
5
6 191 *moneyi*, and *S. palaeindicus* (Fig. 3), and thus we recognize it as an M2.
7
8
9 192

12 193 DISCUSSION

15 194 Four Early Miocene genera of anthracotheres are known from Africa: *Brachyodus*,
16
17
18 195 *Sivameryx*, *Afromeryx*, and *Jaggermeryx*. The distribution of the species of these genera
19
20 196 suggests that African anthracotheres dispersed from Africa to Eurasia, while Eurasian
21
22
23 197 anthracotheres dispersed to Africa. However, the exact pathways enabling such dispersals are
24
25 198 unknown. *Jaggermeryx naida* is a monospecific genus identified only from dentaries and lower
26
27
28 199 dentition found at Wadi Moghra in Egypt (Miller et al., 2014). As such, direct comparisons with
29
30 200 HUJI KJ 31 are impossible. However, *J. naida* differs from known lower dentition of *Sivameryx*
31
32 201 by its bunodont rather than selenodont dentition and overall greater size (Miller et al., 2014). *J.*
33
34
35 202 *naida* is an African genus. Miller et al. (2014) suggested that this genus is derived from older
36
37
38 203 African anthracotheres found in Oligocene deposits of the Fayum in Egypt.
39
40

41 204 *Brachyodus* is considered a descendant of *Bothriogenys* from the Oligocene of the
42
43 205 Fayum in Egypt and thus of African origin (Holroyd et al., 2010). *Brachyodus* currently includes
44
45 206 three species in Africa; *B. depreteti* from Wadi Moghara and Siwa in Egypt (Miller et al., 2014;
46
47
48 207 Pickford, 1991), and from Sperrgebiet in Namibia (Pickford, 2008); *B. mogharensis* found only at
49
50
51 208 Wadi Moghra (Miller et al., 2014; Pickford, 1991); and *B. aequatorialis* in various localities in
52
53 209 East Africa (Kalodirr, Rusinga, Loperot, and Locherangan, Kenya, and Moroto, Uganda) (Holroyd
54
55 210 et al., 2010). Records of *Brachyodus* in Eurasia include: *B. onoideus* from Early Miocene deposits
56
57
58
59
60

1
2
3 211 in southern Europe (Portugal, Spain, France; (e.g. [Antunes and Ginsburg, 2010](#); [Orliac et al.,](#)
4
5 212 [2013](#)) and from Middle Miocene deposits in Thailand (Ducroq et al., 2003). [The exact pathway](#)
6
7
8 213 [and timing of the dispersal by *Brachyodus* from Africa into Eurasia is as yet undetermined.](#)
9

10
11 214 *Afromeryx zelteni* is recognized in North Africa (Jebel Zelten, Libya), East Africa (Loperot,
12
13
14 215 Buluk, Ombo, Nachola and Wayondo, Kenya), and in Ghaba, Sultanate of Oman ([Holroyd et al.,](#)
15
16 216 [2010](#); [Pickford, 1991](#); [Thomas et al., 1999](#)). A second species *A. africanus* is known only from
17
18 217 Jebel Zelten in Libya. Two new species *A. grex* and *A. palustris* were recently described from
19
20
21 218 Wadi Moghara ([Miller et al., 2014](#)). No records of *Afromeryx* are known from Eurasia. Although
22
23
24 219 there is disagreement about its exact ancestral relationships (e.g. [Pickford, 1991](#) vs. [Lihoreau and](#)
25
26 220 [Ducroq, 2007](#)), some researchers argue that it is of Eurasian origin ([Holroyd et al., 2010](#);
27
28 221 [Lihoreau and Ducroq, 2007](#); [Pickford, 1991](#)).

29
30
31 222 Three species, [one Asian and two African](#), are currently included in the genus *Sivameryx*.
32
33
34 223 The type species *S. palaeindicus*, known from several sites in India and Pakistan, is similar in size
35
36 224 and morphology to *S. africanus*, found in East and North Africa (e.g. [Holroyd et al., 2010](#);
37
38
39 225 [Lihoreau and Ducroq, 2007](#)). While some prefer to retain them as two geographically distinct
40
41 226 species ([Holroyd et al., 2010](#)), others suggest that there is insufficient morphological evidence
42
43
44 227 to distinguish between the two species and the earlier name *Sivameryx palaeindicus* should
45
46 228 take precedence (Lihoreau and Ducroq, 2007). In addition to *Sivameryx africanus* identified in
47
48
49 229 East Africa (Karungu, Rusinga, Chianda Uyoma, Kalodirr, [Holroyd et al., 2010](#); [Pickford, 1991](#);
50
51 230 [Rowan et al., 2015](#)), and North Africa (Gebel Zelten, [Pickford, 1991](#)), and possibly in Tunisia
52
53
54 231 (Oued Bazina, [Lihoreau, 2003](#)), [the third species](#), *S. moneyi*, is known only from Wadi Moghara
55
56
57
58
59
60

1
2
3 232 in Egypt (Holroyd et al., 2010; Miller et al., 2014). The two African species are regarded as
4
5 233 morphologically indistinct and are only separated by size differences expressed in the length of
6
7
8 234 the mandibular molar row (~80mm in *S. africanus* vs. ~59mm in *S. moneyi*) (Pickford, 1991).
9
10 235 *Sivameryx africanus* and *S. moneyi* are considered migrants from Eurasia to Africa (Holroyd et
11
12
13 236 al., 2010; Lihoreau and Ducroq, 2007; Miller et al., 2014; Pickford, 1991).

16 237 In order to assign HUJI KJ 31 to a species we wanted to determine if it is similar in size to
17
18 238 *S. moneyi* from Wadi Moghra or the larger species *S. palaeindicus* and *S. africanus*. HUJI KJ 31 is
19
20
21 239 an upper molar, but we expect that the maxillary molars will mirror differences in the size of
22
23
24 240 mandibular molars. However, our analysis of the upper molar dimensions of *Sivameryx* from
25
26 241 Asia, East Africa, and North Africa (Fig. 3) does not support such size distinction. In our analysis,
27
28 242 the smallest individuals are specimens assigned to *S. africanus* from Kalodirr (Holroyd et al.,
29
30
31 243 2010; Rowan et al., 2015). At the same time, the *S. moneyi* specimens from Wadi Moghara have
32
33
34 244 a size range as great as the range of upper molars from India, Pakistan, or Gebel Zelten,
35
36 245 attributed to either *S. palaeindicus* or *S. africanus* (Fig. 3). Alternatively, the overlap in size of
37
38 246 the upper molars of *S. moneyi*, *S. africanus*, and *S. palaeindicus* combined with very little
39
40
41 247 morphological variation may indicate that *Sivameryx* is a monospecific genus. A complete
42
43 248 phylogenetic analysis required to examine this alternative is outside the scope of this paper. We
44
45 249 suggest that size alone, at least as expressed via molar size, is not sufficient to distinguish
46
47
48 250 different species of *Sivameryx* without additional material from well-dated localities. We
49
50
51 251 therefore assign the specimen from Israel as *S. palaeindicus* because we cannot separate any of
52
53 252 the species by upper molar size or morphology and the name *S. palaeindicus* takes precedence
54
55 253 in the literature.

1
2
3 254 Regardless whether the genus *Sivameryx* has one or three species, all authors agree that
4
5
6 255 the genus is an Asian immigrant into Africa ([Holroyd et al., 2010](#); [Lihoreau and Ducrocq, 2007](#);
7
8 256 [Miller et al., 2014](#); [Pickford, 1991](#); [Rowan et al., 2015](#)). HUJI KJ 31 is found in the Levantine
9
10 257 Corridor, an area that physically connects the two continents. This discovery of *Sivameryx* in
11
12
13 258 Israel is part of a growing body of evidence (e.g. ctenodactylid rodents: [López-Antoñanzas et al.,](#)
14
15 259 [2016](#)) that mammals exploited this route to migrate between Asia and Africa as early as the
16
17
18 260 Early Miocene.

21 261

24 262

ACKNOWLEDGMENTS

28 263

31 264 This research is supported by ISF Grant #925/16 (RR and RC). AG is supported by a grant from
32
33 265 Midwestern University. [We are very grateful to the two anonymous reviewers for their](#)
34
35
36 266 [thorough and helpful comments and comments from the editor, Dr. M. Sanchez-Villagra, which](#)
37
38 267 [greatly improved the final manuscript.](#) We wish to thank G. Beiner for preparing the material
39
40
41 268 and V. Gutkin for SEM of the specimen. The faunal collection is deposited at the National
42
43 269 Natural History Collection of the Hebrew University of Jerusalem.

46 270

50 271

REFERENCES

53 272

- 1
2
3 273 Andrews, C. W. 1914. On the Lower Miocene Vertebrates from British East Africa, collected by Dr. Felix
4
5 274 Oswald. Quarterly Journal of the Geological Society 70:163-186.
6
7 275 Antoine, P.-O., G. Métais, M. J. Orliac, J. Crochet, L. J. Flynn, L. Marivaux, A. R. Rajpar, G. Roohi, and J.-L.
8
9 276 Welcomme. 2013. Mammalian Neogene biostratigraphy of the Sulaiman Province, Pakistan.
10
11 277 Fossil mammals of Asia: Neogene Biostratigraphy and Chronology. Columbia University Press,
12
13 278 New York:400 – 422.
14
15
16 279 Antunes, M. T., and L. Ginsburg. 2010. The last Anthracothere *Brachyodus onoideus* (Mammalia,
17
18 280 Artiodactyla) from westernmost Europe and its extinction.
19
20
21 281 Bar, O., and E. Zilberman. 2016. Subsidence and conversion of the Dead Sea basin to an inland erosion
22
23 282 base level in the early middle Miocene as inferred from geomorphological analysis of its ancient
24
25 283 western fluvial outlet. *Geomorphology* 261:147 – 161.
26
27
28 284 Bärmann, E. V., and G. E. Rössner. 2011. Dental nomenclature in Ruminantia: Towards a standard
29
30 285 terminological framework. *Mammalian Biology* 76:762–768.
31
32 286 Boisserie, J.-R., F. Lihoreau, M. Orliac, R. E. Fisher, E. M. Weston, and S. Ducrocq. 2010. Morphology and
33
34 287 phylogenetic relationships of the earliest known hippopotamids (Cetartiodactyla,
35
36 288 Hippopotamidae, Kenyapotaminae). *Zoological Journal of the Linnean Society* 158:325-366.
37
38
39 289 Calvo, R. 2000. Stratigraphy and petrology of the Hazeva Formation in the Arava and the Negev:
40
41 290 Implications for the development of the sedimentary basins and the morphotectonics of the
42
43 291 Dead Sea Rift Valley: In *Geology*, Vol. PhD, pp. 113 (in Hebrew, with English abstract). The
44
45 292 Hebrew University in Jerusalem.
46
47
48 293 Calvo, R., and Y. Bartov. 2001. Hazeva Group, southern Israel: New observations, and their implications
49
50 294 for its stratigraphy, paleogeography, and tectono-sedimentary regime. *Israel Journal of Earth*
51
52 295 *Sciences* 50:71 – 99.
53
54
55
56
57
58
59
60

- 1
2
3 296 Cote, S., J. Kingston, A. Deino, A. Winkler, R. Kityo, and L. MacLatchy. 2018. Evidence for rapid faunal
4
5 297 change in the early Miocene of East Africa based on revised biostratigraphic and radiometric
6
7 298 dating of Bukwa, Uganda. *Journal of Human Evolution* 116:95 – 107.
9
10 299 Ducrocq, S., Y. Chaimanee, V. Suteethorn, and J.-J. Jaeger. 2003. Occurrence of the anthracotheriid
11
12 300 *Brachyodus* (Artiodactyla, Mammalia) in the early Middle Miocene of Thailand. *Comptes Rendus*
13
14 301 *Palevol* 2:261-268.
16
17 302 Ducrocq, S., and F. Lihoreau. 2006. The occurrence of bothriodontines (Artiodactyla, Mammalia) in the
18
19 303 Paleogene of Asia with special reference to *Elomeryx*: Paleobiogeographical implications.
20
21 304 *Journal of Asian Earth Sciences* 27:885 – 891.
23
24 305 Evans, E. N., J. A. Van Couvering, and P. Andrews. 1981. Palaeoecology of Miocene sites in western
25
26 306 Kenya. *Journal of Human Evolution* 10:99 – 116.
27
28 307 Fourteau, R. 1918. Contribution a l'etude des vertebres miocenes de l'Egypte. Geological Survey
29
30 308 Department, Ministry of Finance, Egypt, Cairo. 120p.
32
33 309 Goldsmith, N., E. Tchernov, L. Ginsburg, P. Tassy, and J. Van Couvering. 1982. Ctenodactylid rodents in
34
35 310 the Miocene Negev fauna of Israel. *Nature* 296:645 – 647.
36
37 311 Goldsmith, N. F., F. Hirsch, G. M. Friedman, E. Tchernov, B. Derin, E. Gerry, A. Horowitz, and G.
38
39 312 Weinberger. 1988. Rotem mammals and Yeroham crassostreids: stratigraphy of the Hazeva
40
41 313 Formation (Israel) and the paleogeography of Miocene Africa. *Newsletters on Stratigraphy*:73 –
42
43 314 90.
45
46 315 Gvirtzman, G., and B. Buchbinder. 1969. Outcrops of Neogene Formation in the Central and Southern
47
48 316 Coastal Plain, Hashephela and Beer Sheva'Regions, Israel. *Geological Survey of Israel Bulletin*
49
50 317 50:1 – 73.
52
53 318 Holroyd, P., F. Lihoreau, G. Gunnell, E. Miller, L. Werdelin, and W. Sanders. 2010. Anthracotheriidae.
54
55 319 *Cenozoic Mammals of Africa*. University of California Press, Berkeley:843 – 851.
56
57
58
59
60

- 1
2
3 320 Leakey, M., A. Grossman, M. Gutiérrez, and J. G. Fleagle. 2011. Faunal change in the Turkana Basin
4
5 321 during the late Oligocene and Miocene. *Evolutionary Anthropology: Issues, News, and Reviews*
6
7 322 20:238 – 253.
8
9
10 323 Leidy, J. 1869. The extinct mammalian fauna of Dakota and Nebraska including an account of some allied
11
12 324 forms from other localities, together with a synopsis of the mammalian remains of North
13
14 325 America. *Journal of the Academy of Natural Sciences of Philadelphia*, series 2 7:1-472.
15
16 326 Lihoreau, F. 2003. *Systématique et paléoécologie des Anthracotheriidae [Artiodactyla; Suiformes] du*
17
18 327 *mio-pliocène de l'ancien monde: implications paléobiogéographiques*. Ph.D. Thesis, Université
19
20 328 de Poitiers, Poitiers, France, 395pp.
21
22
23 329 Lihoreau, F., L. Alloing-Séguier, P.-O. Antoine, J.-R. Boisserie, L. Marivaux, G. Métails, and J.-L.
24
25 330 Welcomme. 2016. Enamel microstructure defines a major Paleogene hippopotamoid clade: the
26
27 331 Merycopotamini (Cetartiodactyla, Hippopotamoidea). *Historical Biology*:1 – 11.
28
29
30 332 Lihoreau, F., and S. Ducrocq. 2007. Family Anthracotheriidae; pp. 89 – 105 in D. R. Prothero, and S. E.
31
32 333 Foss (eds.), *The evolution of artiodactyls*. The Johns Hopkins University Press, Baltimore, MD.
33
34 334 López-Antoñanzas, R., V. Gutkin, R. Rabinovich, R. Calvo, and A. Grossman. 2014. The rodent fauna from
35
36 335 the Early Miocene of the Rotem Basin (Israel): African, Asian, both or neither. *Journal of*
37
38 336 *Vertebrate Paleontology* 34 (suppl.):170.
39
40
41 337 López-Antoñanzas, R., V. Gutkin, R. Rabinovich, R. Calvo, and A. Grossman. 2016. A Transitional Gundi
42
43 338 (Rodentia: Ctenodactylidae) from the Miocene of Israel. *PLoS One* 11:e0151804.
44
45
46 339 Lydekker, R. 1877. Notices of new and rare Mammals from the Siwaliks. *Records of the geological Survey*
47
48 340 of India 10:76-83.
49
50 341 Miller, E. R., G. F. Gunnell, M. A. Gawad, M. Hamdan, A. N. El-Barkooky, M. T. Clementz, and S. M.
51
52 342 Hassan. 2014. Anthracotheres from Wadi Moghra, early Miocene, Egypt. *Journal of Paleontology*
53
54 343 88:967 – 981.
55
56
57
58
59
60

- 1
2
3 344 Montgelard, C., F. M. Catzeflis, and E. Douzery. 1997. Phylogenetic relationships of artiodactyls and
4
5 345 cetaceans as deduced from the comparison of cytochrome b and 12S rRNA mitochondrial
6
7 346 sequences. *Molecular Biology and Evolution* 14:550-559.
- 8
9
10 347 Orliac, M. J., P.-O. Antoine, A.-L. Charruault, S. Hervet, F. Prodeo, and F. Duranthon. 2013. Specialization
11
12 348 for amphibiosis in *Brachyodus onoideus* (Artiodactyla, Hippopotamoidea) from the Early
13
14 349 Miocene of France. *Swiss Journal of Geosciences* 106:265-278.
- 15
16 350 Patnaik, R. 2013. Indian Neogene Siwalik mammalian biostratigraphy: an overview. *Fossil mammals of*
17
18 351 *Asia: Neogene Biostratigraphy and Chronology*. Columbia University Press, New York:423 – 444.
- 19
20
21 352 Pickford, M. 1991. Revision of the Neogene Anthracotheriidae of Africa. *The Geology of Libya*:1491 –
22
23 353 1525.
- 24
25 354 Pickford, M. 2008. Anthracotheriidae from the Early Miocene deposits of the northern Sperrgebiet,
26
27 355 Namibia. *Geology and palaeobiology of the Northern Sperrgebiet, Namibia*. Geological Survey of
28
29 356 Namibia, *Memoir* 20:343-348.
- 30
31
32 357 Rabinovich, R., A. Grossman, H. Ginat, Y. Avni, and R. Calvo. 2014. Newly discovered Miocene
33
34 358 proboscideans in the southern Levant. *Journal of Vertebrate Paleontology* 34 (suppl.):210.
- 35
36
37 359 Rowan, J., B. Adrian, and A. Grossman. 2015. The first skull of *Sivameryx africanus* (Anthracotheriidae,
38
39 360 Bothriodontinae) from the early Miocene of East Africa. *Journal of Vertebrate Paleontology* 35:3
40
41 361 e928305.
- 42
43 362 Sanders, W. j., E. Gheerbrant, J. M. Harris, H. Saegusa, and C. Delmer. 2010. Proboscidea; pp. 161 – 251
44
45 363 in L. Werdelin, and W. J. Sanders (eds.), *Cenozoic Mammals of Africa*. University of California
46
47 364 Press.
- 48
49
50 365 Sanders, W. J., and E. R. Miller. 2002. New proboscideans from the early Miocene of Wadi Moghara,
51
52 366 Egypt. *Journal of Vertebrate Paleontology* 22:388 – 404.
- 53
54
55 367 Savage, R., and E. Tchernov. 1968. Miocene mammals of Israel. *Proc Geol Soc London* 1648:98 – 101.
- 56
57
58
59
60

- 1
2
3 368 Savage, R. J., P. C. Dixit, and D. Murty. 1977. On an anthracothere upper molar from Ladakh, Kashmir.
4
5 369 Journal of the Palaeontological Society of India 20:219 – 223.
6
7 370 Sehgal, R., and A. Bhandari. 2014. Miocene mammals from India: present status and future prospects.
8
9 371 Indian Miocene: a geodynamic and chronological framework for palaeobiota, sedimentary
10
11 372 environments and palaeoclimates. Palaeontol. Soc. India Spec. Publ 5:199 – 212.
12
13 373 Steinitz, G., Y. Bartov, and J. Hunziker. 1978. K-Ar age determinations of some Miocene–Pliocene basalts
14
15 374 in Israel: their significance to the tectonics of the Rift Valley. Geological Magazine 115:329 – 340.
16
17 375 Tchernov, E., L. Ginsburg, P. Tassy, and N. Goldsmith. 1987. Miocene mammals of the Negev (Israel).
18
19 376 Journal of Vertebrate Paleontology 7:284 – 310.
20
21 377 Thomas, H., R. Jack, S. Sen, M. Pickford, E. Gheerbrant, Z. Al-Sulaimani, and S. Al-Busaidi. 1999.
22
23 378 Oligocene and Miocene terrestrial vertebrates in the Southern Arabian peninsula (Sultanate of
24
25 379 Oman) and their geodynamic and paleogeographic settings; pp. 430-442 in P. J. Whybrow, and
26
27 380 A. Hill (eds.), Fossil vertebrates of Arabia. Yale University Press, New Haven, CT.
28
29
30
31
32
33 381 Zilberman, E., and R. Calvo. 2013. Remnants of Miocene fluvial sediments in the Negev Desert, Israel,
34
35 382 and the Jordanian Plateau: Evidence for an extensive subsiding basin in the northwestern
36
37 383 margins of the Arabian plate. Journal of African Earth Sciences 82:33 – 53.
38
39
40
41 384
42
43
44 385 Submitted July 14, 2018; accepted Month DD, YYYY
45
46
47 386
48
49
50 387
51
52
53 388
54
55
56
57
58
59
60

1
2
3 3894
5
6 3907
8
9 391

FIGURE CAPTIONS

10
11
12 392 FIGURE 1. Location map of the Kamus Junction (KJ) locality in the Yamin Plain, northern Negev,
13
14
15 393 Israel.

16
17
18 394 **A.** General location of northern Negev, Israel.

19
20
21 395 **B.** Hazeva Formation outcrops in the northern Negev. Kamus Junction area is marked by a
22
23
24 396 blue star.

25
26
27 397 **C.** The Hazeva Formation fills the Yamin Plain with all of its members. In the Kamus
28
29 398 Junction area the upper parts of Zefa Member are overlain by clastic units of the Rotem
30
31 399 Member. Small unconformity separates the lower and upper parts of the Rotem
32
33
34 400 Member. Green dot marks the location of the upper level of KJ site where HUJI KJ 31
35
36 401 was found.

37
38
39 402 **D.** Topographic elevation of KJ site where HUJI KJ 31 was found (Green dot).

40
41
42 403 **E.** Columnar stratigraphic section in the Kamus Junction locality.

43
44
45
46 404 [Intended for Full page width]

47
48
49 405

50
51
52 406 FIGURE 2. SEM and schematic drawing of HUJI KJ 31—M2 of *Sivameryx palaeindicus* in occlusal
53
54
55 407 view. Arrow on schematic indicates the paraconule.

1
2
3
4
5
6
7
8
9
10
11
12
13
14
15
16
17
18
19
20
21
22
23
24
25
26
27
28
29
30
31
32
33
34
35
36
37
38
39
40
41
42
43
44
45
46
47
48
49
50
51
52
53
54
55
56
57
58
59
60

408 [Intended for 2/3 page width]

409

410 FIGURE 3. Scatter plot of upper molars of *Sivameryx* spp.

411 KEY: Triangles = M1, Squares = M2, Trapezoid = M3, Cross = HUJI KJ 31

412 Grey fill = *S. moneyi*, Dark fill = *S. africanus*, White fill = *S. palaeindicus*

413 Measurements listed in Table 1

414 [Intended for 2/3 page width]

415

416

TABLE 1. Measurements of *Sivameryx* spp. Upper molars

Specimen No.	MD	BL	Tooth position	Reference	Site
KJ 31	19.8	21.8	M2	This paper	Kamus Junction
<i>Sivameryx moneyi</i>					
CUWM 64AB	19.92	18.27	M1	Miller et al. 2014	Wadi Moghara
CUWM 64AB	23.08	21.18	M2	Miller et al. 2014	Wadi Moghara
CUWM 64AB	23.44	22.46	M3	Miller et al. 2014	Wadi Moghara
CUWM 70	17.5	17.5	M1	Miller et al. 2014	Wadi Moghara
CUWM 70	22.11	21.55	M2	Miller et al. 2014	Wadi Moghara
DPC 4066	21.47	22.34	M2	Miller et al. 2014	Wadi Moghara
DPC 4066	24.04	24.86	M3	Miller et al. 2014	Wadi Moghara
DPC 5979	20.71	20.89	M2	Miller et al. 2014	Wadi Moghara
DPC 6243	15.5	16.35	M1	Miller et al. 2014	Wadi Moghara
DPC 6243	23.12	20.81	M2	Miller et al. 2014	Wadi Moghara
DPC 6289	21.1	21.32	M3	Miller et al. 2014	Wadi Moghara
DPC 7659	25.35	22.89	M3	Miller et al. 2014	Wadi Moghara

TABLE 1. (Continued)

DPC 17685	20.69	20.08	M2	Miller et al. 2014	Wadi Moghara
DPC 17685	22.23	22.12	M3	Miller et al. 2014	Wadi Moghara
DPC 21506	27.49	30.03	M3	Miller et al. 2014	Wadi Moghara
<i>Sivameryx africanus</i>					
WK 18129	12.4	14.7	M1	Rowan et al. 2015	Kalodirr
WK 18129	11.6	15.5	M1	Rowan et al. 2015	Kalodirr
WK 18129	13.6	18.3	M2	Rowan et al. 2015	Kalodirr
WK 18129	14.6	18.7	M2	Rowan et al. 2015	Kalodirr
WK 18129	19.9	20.3	M3	Rowan et al. 2015	Kalodirr
WK 18129	16.6	18.9	M3	Rowan et al. 2015	Kalodirr
WK 17109	10.9	11.9	M1	Holroyd et al. 2010	Kalodirr
<i>S. africanus</i>	22.9	20.8	M2	Lihoreau et al. 2016	Gebel Zelten, or Rusinga or Karungu

Sivameryx palaeindicus

Ladakh Molar	24	26	M2	Savage et al. 1977	Ladakh
B82	22	25	?M3	Savage et al. 1977	Laki Hills
B82	20.5	22.5	?M2	Savage et al. 1977	Laki Hills

TABLE 1. (Continued)

M12738	24	25	M3	Savage et al. 1977	Dera Bugti
B482	19	20	?M1	Savage et al. 1977	Bugti Hills
B482a	21	22.5	?M2	Savage et al. 1977	Bugti Hills
Y238	19	18	M1	Lihoreau 2003	Potwar Y27926

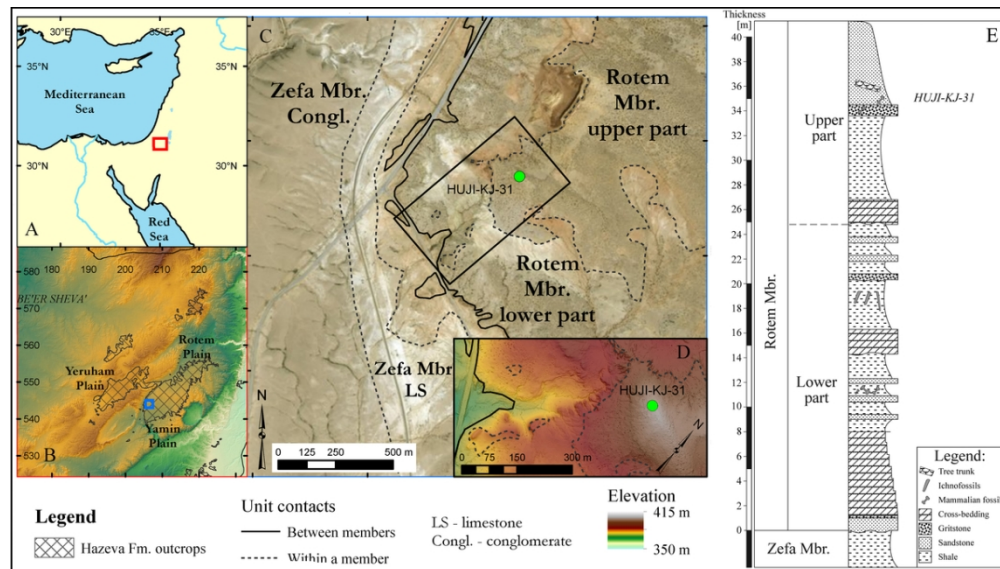


FIGURE 1. Location map of the Kamus Junction (KJ) locality in the Yamin Plain, northern Negev, Israel.

A. General location of northern Negev, Israel.

B. Hazeva Formation outcrops in the northern Negev. Kamus Junction area is marked by a blue star.

C. The Hazeva Formation fills the Yamin Plain with all of its members. In the Kamus Junction area the upper parts of Zefa Member are overlain by clastic units of the Rotem Member. Small unconformity separates the lower and upper parts of the Rotem Member. Green dot marks the location of the upper level of KJ site where HUJI KJ 31 was found.

D. Topographic elevation of KJ site where HUJI KJ 31 was found (Green dot).

E. Columnar stratigraphic section in the Kamus Junction locality.

103x58mm (300 x 300 DPI)

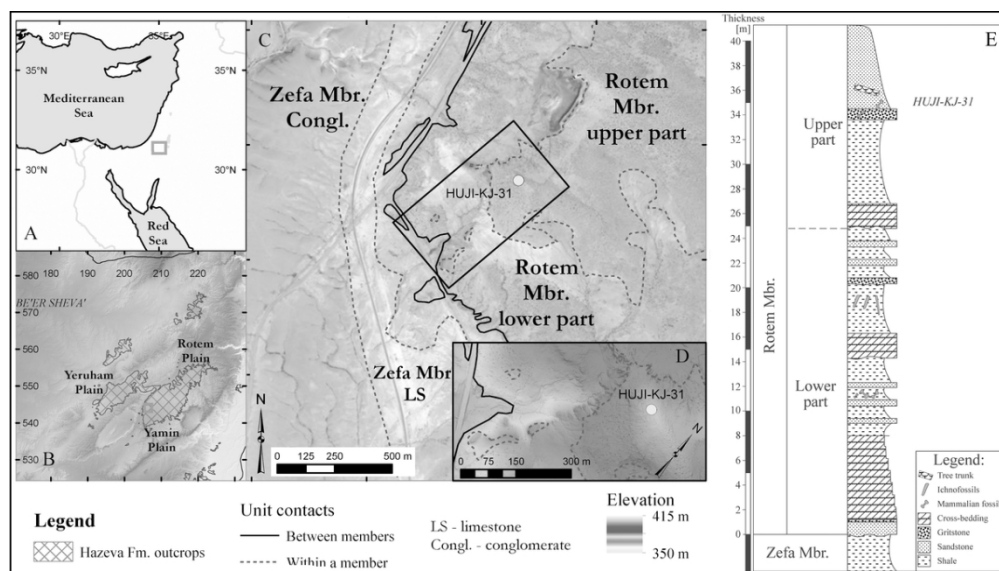


FIGURE 1. Location map of the Kamus Junction (KJ) locality in the Yamin Plain, northern Negev, Israel.

A. General location of northern Negev, Israel.

B. Hazeva Formation outcrops in the northern Negev. Kamus Junction area is marked by a blue star.

C. The Hazeva Formation fills the Yamin Plain with all of its members. In the Kamus Junction area the upper parts of Zefa Member are overlain by clastic units of the Rotem Member. Small unconformity separates the lower and upper parts of the Rotem Member. Green dot marks the location of the upper level of KJ site where HUJI KJ 31 was found.

D. Topographic elevation of KJ site where HUJI KJ 31 was found (Green dot).

E. Columnar stratigraphic section in the Kamus Junction locality.

103x58mm (300 x 300 DPI)

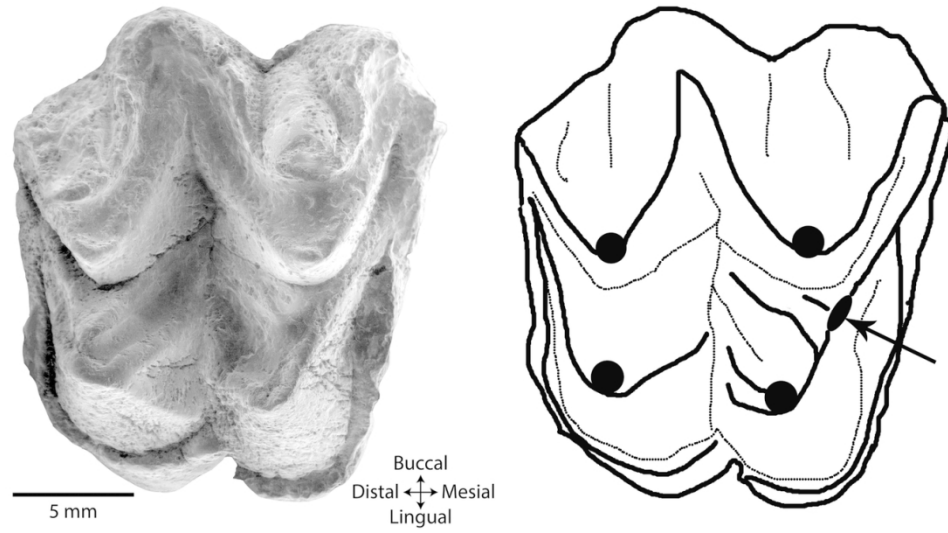


FIGURE 2. SEM and schematic drawing of HUJI KJ 31—M2 of *Sivameryx palaeindicus* in occlusal view. Arrow on schematic drawing indicates the paraconule.

119x64mm (300 x 300 DPI)

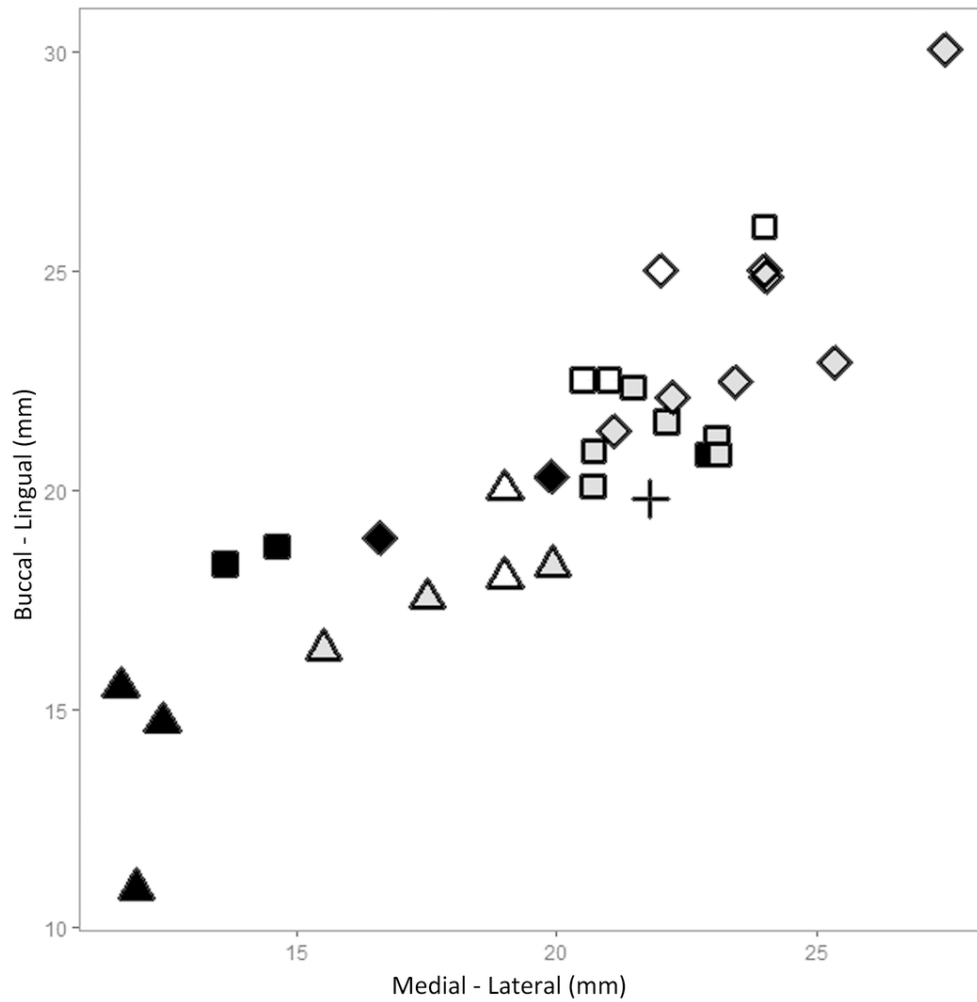


FIGURE 3. Scatter plot of upper molars of *Sivameryx* spp.
 KEY: Triangles = M1, Squares = M2, Trapezoid = M3, Cross = HUJI KJ 31
 Grey fill = *S. moneyi*, Dark fill = *S. africanus*, White fill = *S. palaeindicus*
 Measurements listed in Table 1

90x90mm (300 x 300 DPI)